Journal of Photochemistry and Photobiology B: Biology 137 (2014) 31–38

Contents lists available at ScienceDirect

Journal of Photochemistry and Photobiology B: Biology

journal homepage: www.elsevier.com/locate/jphotobiol

Effects of mutual shading on the regulation of photosynthesis in field-grown sorghum

Tao Li [a,b], Li-Na Liu [a], Chuang-Dao Jiang [a,*], Yu-Jun Liu [b], Lei Shi [a,*]

[a] Key Laboratory of Plant Resources, Institute of Botany, Chinese Academy of Sciences, Beijing 100093, China
[b] College of Biological Sciences and Biotechnology, Beijing Forestry University, Beijing 100083, China

ARTICLE INFO

Article history:
Received 13 December 2013
Received in revised form 14 April 2014
Accepted 24 April 2014
Available online 5 May 2014

Keywords:
Sorghum
Mutual shading
Photosynthesis
Leaf structure
Photoprotection

ABSTRACT

In the field, close planting inevitably causes mutual shading and depression of leaf photosynthesis. To clarify the regulative mechanisms of photosynthesis under these conditions, the effects of planting density on leaf structure, gas exchange and proteomics were carefully studied in field-grown sorghum. In the absence of mineral deficiency, (1) close planting induced a significant decrease in light intensity within populations, which further resulted in much lower stomatal density and other anatomical characteristics associated with shaded leaves; (2) sorghum grown at high planting density had a lower net photosynthetic rate and stomatal conductance than those grown at low planting density; (3) approximately 62 protein spots changed their expression levels under the high planting density conditions, and 22 proteins associated with photosynthesis were identified by mass spectrometry. Further analysis revealed the depression of photosynthesis caused by mutual shading involves the regulation of leaf structure, absorption and transportation of CO_2, photosynthetic electron transport, production of assimilatory power, and levels of enzymes related to the Calvin cycle. Additionally, heat shock protein and oxygen-evolving enhancer protein play important roles in photoprotection in field-grown sorghum. A model for the regulation of photosynthesis under mutual shading was suggested based on our results.

1. Introduction

Photosynthesis is the basis of crop growth and yield formation. Light not only acts as the driving force of photosynthesis, but also affects the structure and function of photosynthetic apparatus. Therefore, light plays an important role in photosynthesis and crop yield [1,2]. Leaves differ greatly in structure and physiology under high- and low-light conditions [3,4]. Generally, sun leaves developed under high light are smaller and thicker, with more developed palisade tissue, higher stomatal density, and thinner granal stacks compared to shade leaves [4,5]. In addition to leaf morphology and structure, the series of physiological and biochemical reactions are also adjusted considerably [3]. Sun leaves have lower chlorophyll content, yet have higher quantities of electron transfer carriers and ribulose-1,5-bisphosphate carboxylase/oxygenase (Rubisco) than shade leaves based on leaf area [2,3,5,6]. Accordingly, sun leaves have a higher photosynthetic capacity per leaf area. Conversely, shade leaves exhibit a lower photosynthetic capacity.

Though light is very important for photosynthesis, too much light can also damage the photosynthetic apparatus. To avoid the photodamage caused by high light, plants have developed several mechanisms to deal with excessive irradiance [7–9]. Among these photoprotective mechanisms, one of the most important is thermal dissipation relying on xanthophyll cycle [10]. Despite the existence of this mechanism for releasing excessive excited energy, the production of reactive oxygen species is still unavoidable during photosynthesis, especially under strong irradiance. To counteract the toxicity of reactive oxygen species, plants have developed a highly efficient antioxidant enzymic defense system [11], mainly comprising superoxide dismutase, ascorbate peroxidase, catalase, peroxidase, and glutathione reductase. Many studies have proved that sun leaves are insensitive to strong light, while shade leaves grown under low light have a weak photoprotection capacity and enhanced sensitivity to high light [4,9]. However, most of the evidence is derived from simulation experiments, in which there were striking differences in light intensities between plant growth and treatment. For instance, light intensity during plant growth was 150 $\mu mol\ m^{-2}\ s^{-1}$, while that used to induce photoinhibition was 1800 $\mu mol\ m^{-2}\ s^{-1}$, and so on [9,11]. Such studies may greatly assist in elucidating photoprotective mechanisms under conditions of extremely strong light, but might not reflect the actual light acclimation strategies of crops in the field.

* Corresponding authors. Tel.: +86 10 62836657.
E-mail addresses: jcdao@ibcas.ac.cn (C.-D. Jiang), shilei67@ibcas.ac.cn (L. Shi).

http://dx.doi.org/10.1016/j.jphotobiol.2014.04.022
1011-1344/

In practice, planting density is very important for crop production [12,13]. Close planting of crops always causes mutual shading among individuals and inevitably a depression in leaf photosynthesis [6]. In this situation, not only the light intensity, but also the spectrum of light is changed as a result of mutual shading [5,14]. In fact, variations in both light intensity and the spectral components have a major influence on photosynthesis [5,15]. However, most previous studies concerning the response of crops to shading have mainly focused on artificial shading in the field [1,2]. Artificial shading with shade nets or screens does not change the components of the spectrum [14]. Evidently, there are distinct differences between artificial shading and mutual shading in the field. Therefore, the mechanisms of decreases in photosynthesis caused by mutual shading may be different when it comparing with artificial shading under field conditions.

Sorghum, a typical C4 plant, is one of the most important crops globally, with a very high photosynthetic rate and large biomass production. To clarify the regulative mechanisms of photosynthesis in the field, the effects of mutual shading among individuals on gas exchange, chlorophyll fluorescence, leaf structure and proteomics were carefully investigated. This study provides new insight into photosynthetic regulation in field.

2. Materials and methods

2.1. Plant growth and experiment design

The experiment was conducted at the Botanical Institute of Chinese Academy of Sciences, Beijing (39°28′–41°25′N and 115°25′–117°30′E), in 2012–2013, in a semi-humid, continental, and monsoon climate. Sorghum (*Sorghum bicolor* L. cv 'Liaoza 12') seeds were imbibed on wet paper for 1 day and the germinated seeds were sown in columniform downspouts (0.16 m in diameter and 0.75 m in height) filled with culture media (peat:loess = 1:1; the mixed soil in each downspout contained 360 g moderate organic manure and 1.43 g available *N*), at the beginning of May, 2012 and 2013. The bottom of each columniform downspout was sealed with a nutrition bowl and embedded in the field under one of two planting densities (5 and 36 plants m^{-2}). There was one seedling per downspout, as shown in Fig. 1. Nutrition and water were supplied in sufficient quantities per plant throughout the experiment; therefore, avoiding potential nutrient and drought stress. During the experiments, plots (2 m × 2 m) were selected randomly. The fifth leaf (from top to bottom) was used for all measurements in this study.

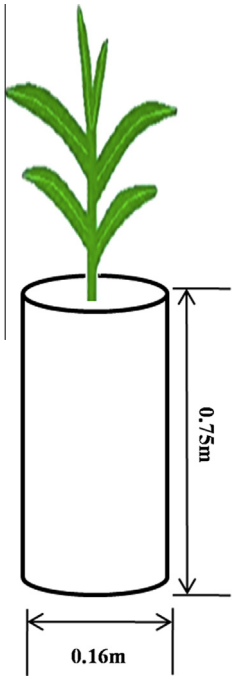

Fig. 1. Experimental design in the field.

2.2. Measurement of plant growth

Plant height, stem diameter, length and width of each leaf (ten replicates for each planting density) were determined using a straightedge rule and vernier caliper. Leaf area was measured using a leaf area meter (AM100; ADC, UK). Specific leaf weight was calculated based on leaf area and leaf dry weight.

On a clear day, the diurnal variations in light intensity and air temperature were obtained using a quantum meter (QMSS; Photosynthetic Photo Flux, USA) and thermometer, respectively.

2.3. Measurement of gas exchange

Gas exchange analysis was performed in a leaf chamber with a CO_2 concentration of 380 μmol mol^{-1}, 80% relative humidity under an irradiance of either 600 or 1200 μmol m^{-2} s^{-1}, using a gas exchange system (CIRAS-2; PP-Systems, UK). Net photosynthetic rate (P_n) and stomatal conductance (G_s) were determined before 11:00 on a sunny day. The P_n and G_s were recorded when CO_2 uptake was steady and ten leaves were measured for each planting density.

2.4. Measurement of chlorophyll a fluorescence

Chlorophyll *a* fluorescence was measured using a fluorimeter (Handy PEA; Hansatech, UK). Fully dark-adapted leaves (10 h) were used to determine F_v/F_m (where F_v is the variable and F_m is the maximum Chl fluorescence yield) at 06:00. After the initial Chl fluorescence yield (F_o) was measured, a 1-s pulse of saturating red light (3500 μmol m^{-2} s^{-1}) was applied to obtain F_m. The result for F_v/F_m was calculated as $(F_m–F_o)/F_m$, in which F_v is defined as $F_m–F_o$ [16]; F_v/F_m was also determined at 14:00 and 18:00 after dark adaption for 20 min of 20 leaves measured in each treatment.

2.5. Measurement of chlorophyll content

Twenty leaf discs (5.652 cm^2) were cut from the middle part of each leaf lamina with a puncher (6 mm in diameter). Samples for chlorophyll pigment analysis were extracted using 80% acetone, and absorbance measurements were made using a spectrophotometer (UV-8000S; China) at 663 nm and 646 nm. Chlorophyll content was calculated according to the method of Porra et al. [17]; five replicates were measured for each treatment.

2.6. Measurement of stomatal density and leaf anatomical structure

Stomatal density was measured followed the method of Coupe et al. [18]. Nail polish was applied to dental imprints to obtain a replica of the leaf surface. The replica was observed under a light microscope (Nikon-E800; Japan), and photographed using a digital camera (BH-2; Olympus, Japan). The number of stomata was counted in 20 fields of view using six marked leaves from each treatment.

As described by Jiang et al. [4], a leaf segment (2 mm × 2 mm) without major veins was fixed at 4 °C in 3% glutaraldehyde in 0.1 M cacodylate buffer (pH 7.2), and then treated with 1% osmium tetroxide overnight at 4 °C. The fixed segment was dehydrated in a graded acetone series and embedded in Spurr's resin (Ladd). Light

microscopy (Nikon-E800; Japan) was carried out with a 1-μm thick transverse section of the leaf cut with a glass knife on an ultramicrotome (Leica Ultracut R, Germany) and stained with 0.5% toluidine blue. Light micrographs were obtained using a digital camera (BH-2; Olympus, Japan). Measurements of leaf thickness, cross-sectional area of the vascular bundle, and contact area of the bundle sheath cells [19] were obtained using Photoshop software; 20 different positions were measured in each segment.

2.7. Proteomic determination

2.7.1. Preparation, extraction, and quantitation of total protein

Leaf samples were immediately weighed and immersed in liquid nitrogen, and stored at −80 °C for proteomic analysis at Beijing Protein Innovation Co., Ltd. (Beijing Genomics Inst.; BGI). A leaf sample (1 g) from each replicate was ground into a fine powder with 10% (w/v) polyvinylpolyrrolidone (PVPP) and liquid nitrogen in a pre-chilled mortar. The powder was then incubated in a pre-chilled centrifuge tube to extract protein using the TCA/acetone method [20]. After vacuum drying, the resulting proteins were dissolved in a lysis buffer (7 M urea, 2 M thiourea, 2% (w/v) CHAPS, 20 mM Tris–HCl, pH8.8), and then subjected to ultrasound for 5 min in an ice bath (pulse on 2 s, pulse off 3 s, power 180 W). The supernatant was collected by centrifugation at 20,000×*g* for 30 min at 15 °C. The protein standard curve was derived by using the 2-D Quant-kit method to quantify protein; the protein concentration was determined [21].

2.7.2. Two-dimensional polyacrylamide gel electrophoresis and gel scanning

The proteins extracted from the sorghum leaves were diluted with a 450 μl rehydration buffer containing 50 mM DTT and 0.8% (v/v) immobilized pH gradient (IPG) buffer [22], and was then mixed thoroughly and centrifuged at 20,000×g for 10 min at 10 °C. The samples were prepared three times using two-dimensional electronphoresis; isoelectric focusing was performed using an IEF-strip holder of 24 cm length, pH4–7. After electrofocusing, each sample was equilibrated in 1% DTT and 2.5% iodoacetamide equilibrium buffers for 15 min for 15 min, respectively. The strips were then immediately used to perform second-dimension separation in 12.5% gel and SDS–PAGE procedure at 20 °C, until the bromophenol turned blue, as an indicator that the gel was completely depleted. Gels were stained with Coomassie Brilliant Blue G-250. Subsequently, images were obtained by scanning the stained gels and saved as a TIF image for further analysis (Image Master 2D platinum 5.0).

2.7.3. Image analysis, protein identification, and database search

Proteins were analyzed according to the methods of Fan et al. [23]; only those spots that reproducibly changed in abundance by more than twofold and passed the significance test ($p \leqslant 0.05$) were termed differentially expressed proteins and selected for protein identification. Each spot to be analyzed was excised from a gel, placed into a 1.5 ml centrifuge tube, and numbered. After proteolysis, the spots were tested using MALDI TOF/TOF. After the first mass-spectrometry, three precursor ions were selected for a second quassation. Some broken fragments were observed at the top of the marked mass spectrum, and its mass-to-charge ratio was shown in the second mass-spectrometry; this could then be submitted to MASCOT (Matrix-Science, London, UK) server for the search. According to the score, results for the *E* value, protein sequence coverage, peak intensity of matching peptides, experimentally calculated PI, relative molecular weight, and other factors were retrieved and analyzed.

2.8. Statistics

Data were compared with the Independent-Samples *T* test using SPSS (version 11.5), at the 0.05 and 0.01 significance levels. The graphics program SigmaPlot (version 10.0) was used to create artwork.

3. Results

3.1. Effects of mutual shading on light intensity and air temperature

On sunny days, the maximum light intensity value was approximately 1343 μmol m^{-2} s^{-1} at low planting density, while at high planting density it only reached 390 μmol m^{-2} s^{-1} at noon (Fig. 2A). The daily changes in temperature within the population were consistent with light intensity (Fig. 2B). The maximum temperature under the low and high planting densities occurred at 14:00, and was 36.3 °C and 32.8 °C, respectively. Light intensity and temperature within the sorghum population were clearly lowered significantly by mutual shading under close planting.

3.2. Effects of mutual shading on plant growth and leaf structure

Compared with sorghum grown at a low planting density, sorghum at a high planting density had a higher plant height, while the stem diameter, leaf area of plant, single leaf area, and specific leaf weight were lower (Table 1). Moreover, the stomatal density of leaves grown at the high planting density decreased significantly compared with leaves at low planting density.

In order to further analyze the effects of mutual shading on photosynthetic organs, leaf structure was also studied (Fig. 3, Table 1). Under high planting density, mutual shading caused a marked reduction in leaf thickness, the cross-sectional area of

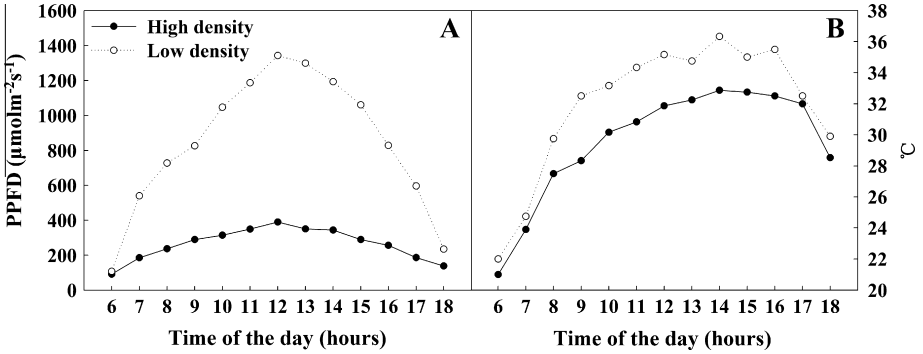

Fig. 2. Effects of planting density on diurnal variations of PPFD and air temperature within the population in field-grown sorghum.

Table 1
Effects of planting density on plant growth and leaf structure.

Trait	High density	Low density
Plant height (cm)	160.3 ± 1.26596aA	141.9 ± 2.14832bB
Stem diameter (cm)	1.5733 ± 0.0434bB	2.055 ± 0.03662aA
Leaf area of plant (cm^2)	3700.5155 ± 172.0550bB	4588.1748 ± 85.28308aA
Single leaf area (cm^2)	325.7009 ± 16.8854bB	417.1068 ± 7.75301aA
Specific leaf weight ($g\ m^{-2}$)	39.146 ± 2.13284bB	45.9726 ± 0.72344aA
Stomatal density (No. mm^{-2})	193.2401 ± 12.6657bA	234.2975 ± 5.2047aA
Leaf thickness (μm)	120.0838 ± 0.54171bB	143.3209 ± 0.7385aA
Cross section area of vascular bundle (μm^2)	1859.8887 ± 136.37233bB	2535.3780 ± 104.10333aA
Contact area of bundle sheath cell ($\mu m\ \mu m^{-1}$)	4.0170 ± 0.04779bA	4.1497 ± 0.02868aA
Chlorophyll content ($mg\ m^{-2}$)	558.2788 ± 6.95045bB	516.4952 ± 4.9053aA

the vascular bundle, and contact area of the bundle sheath cells, when compared to low planting density. Therefore, these changes in the morphological and anatomical structure indicated that sorghum grown at a high planting density developed typical features of shade plants.

3.3. Effects of mutual shading on photosynthetic function

To further explain the leaf responses to mutual shading, we measured chlorophyll content, gas-exchange, and chlorophyll fluorescence. At high planting density, chlorophyll content distinctly increased because of severe mutual shading (Table 1). Values for P_n and G_s at irradiances of 600 and 1200 $\mu mol\ m^{-2}\ s^{-1}$ are shown in Fig. 4. Both P_n and G_s decreased significantly at high compared to low planting density. At the same time, sorghum growing at high planting density exhibited slight photoinhibition at noon (Fig. 5). The serious decline of F_v/F_m in sorghum at low planting density was observed, which mainly due to the depression of F_m and increase in F_o.

3.4. Effects of mutual shading on leaf proteome

To examine changes in the proteome profiling of sorghum leaves subjected to mutual shading, we performed a 2-D gel analysis. Fig. 6 shows the 2-DE profiles of the proteins, of which 62 protein spots showed a significant difference in expression level ($p < 0.05$). A total of 52 proteins were successfully identified by MALDI TOF/TOF from all the differentially expressed proteins (DEPs), and 22 proteins associated with photosynthetic light acclimation are listed in Table 2. These identified proteins could be classified into four categories according to the classification of Fan et al. [23] and Li et al. [22]: light reaction, carbon metabolism, photoreceptor proteins, and photoprotection.

The first category is the light reaction of photosynthesis (Table 2), which is related to electron transport and the formation of assimilatory power. The abundances of putative NADH-plastoquinone oxidoreductase subunit K isoform 1, ferredoxin-NADP reductase (FNR), ferredoxin (Fd), oxygen-evolving enhancer protein 1, and ATP synthase beta subunit were all upregulated in leaves grown at low planting density, but downregulated in leaves at high planting density.

The second category is correlated with carbon metabolism enzymes. Table 2 shows that the abundance of malate dehydrogenase, ribulose-1,5-bisphosphate carboxylase/oxygenase small subunit, triosephosphate isomerase, phosphoribulokinase, sedoheptulose bisphosphatase1 (SBPase), sucrose synthase (SS), and granule-bound starch synthase I (GBSS) were all upregulated in leaves grown at low planting density, but the expression abundance of ribulose-1,5-bisphosphate carboxylase/oxygenase large subunit was downregulated (Table 2).

The third category is related to photoreceptor proteins. Of these, cryptochrome 2 was upregulated in leaves grown at low planting density, while the expression of phytochrome C was downregulated (Table 2).

The fourth category comprises proteins associated with photoprotection. The abundances of chloroplast heat shock protein 70 and oxygen-evolving enhancer protein 1 were both upregulated in leaves grown at low planting density, but downregulated in leaves grown at high planting density (Table 2). Furthermore, the abundance of oxygen-evolving enhancer protein 1 at low planting density was over six times as high as at high planting density (Table 2).

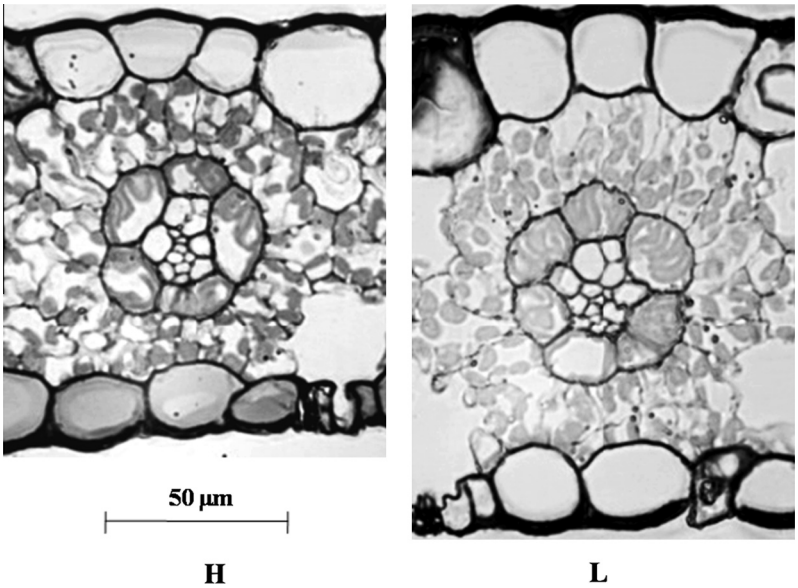

Fig. 3. Light micrographs of cross-sections of leaves grew under low (*L*) and high (*H*) planting densities.

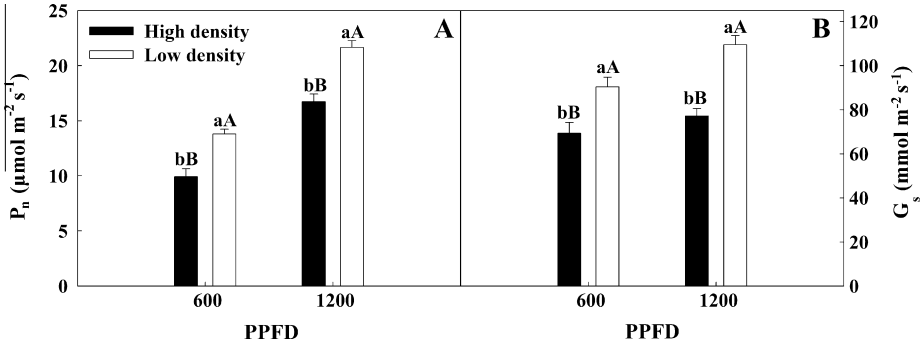

Fig. 4. Effects of planting density on net photosynthetic rate (P_n) and stomatal conductance (G_s). Measurements were made in a leaf chamber with CO_2 concentration of 380 μmol mol^{-1}, 80% relative humidity under irradiance of 600 and 1200 μmol m^{-2} s^{-1}. Values are means ± SE, capital and lowercase letters represent the statistically significant differences at $P < 0.01$ and $P < 0.05$ level, respectively, similarly hereinafter.

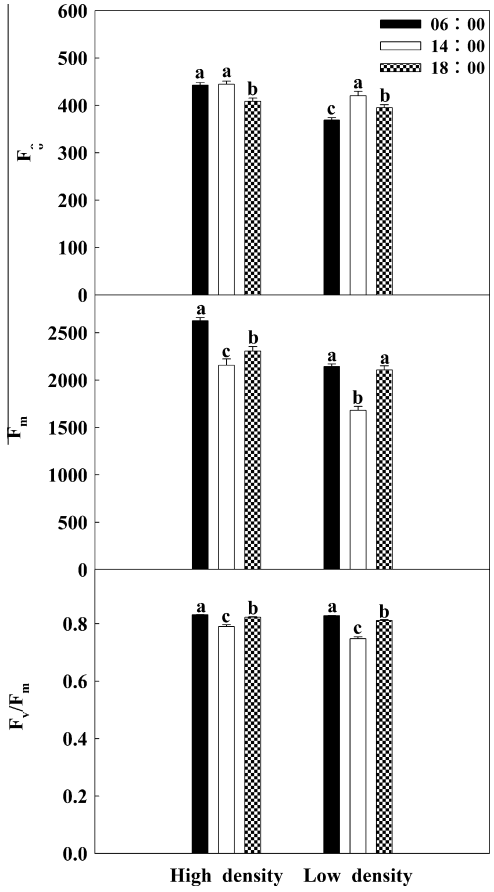

Fig. 5. Effects of planting density on chlorophyll fluorescence. Chlorophyll fluorescence was determined after dark adaption at 6:00, 14:00 and 18:00, respectively.

4. Discussion

4.1. Effects of mutual shading on photosynthetic capacity

In this study, close planting of sorghum caused severe mutual shading, as reflected in the striking decline of irradiance within populations (Fig. 2A). Therefore, sorghum grown at a high planting density developed shade leaves (Fig. 3 and Table 1). We know that leaf morphological characteristics and anatomical structure play key roles in the regulation of photosynthetic capacity, providing a structural framework for the diffusion of gases and the optimization of the photosynthetic function [4,18,24]. Theoretically, higher stomatal density and thicker leaves, as well as a more rapid metabolite transfer between the mesophyll and bundle sheath cells, tend to favor a higher photosynthetic rate [25]. Accordingly, under mutual shading the decreased stomatal density, leaf thickness, cross-sectional area of the vascular bundle, and contact area of the bundle sheath cells, all features of morphology and anatomical structure of leaves (Table 1), may be partially responsible for depressing photosynthetic capacity.

In addition, decreased photosynthesis was found not only to result from significant changes in the morphological characteristics and anatomical structure, but also in functional proteins (Table 2). Generally, CO_2 enters the mesophyll through stomata on the surfaces of leaves, which is highly sensitive to the light environment. In the present study, mutual shading under conditions of high planting density led to a significant decrease in stomatal density and G_s (Fig. 4 and Table 1). Therefore, the exchange of CO_2 through stomata may be restricted. For a typical C4 plant, such as sorghum, ambient CO_2 is initially fixed as a four-carbon acid (malate, Mal) in mesophyll cells through PEPCase. The malate is then transferred into the bundle sheath cells. Thereafter, decarboxylation of malate through a decarboxylating enzyme yields a high concentration of CO_2 around Rubisco that facilitates its assimilation via the Calvin cycle. The decreased abundance of malate dehydrogenase in plants grown at high planting density indicated that the rate of CO_2 released into the bundle sheath cells via malate decarboxylation might have been slowed down. Mutual shading therefore resulted in a decrease in the uptake and transportation of CO_2 in photosynthesis.

Additionally, although a distinct increase in chlorophyll content was observed due to mutual shading (Table 1), the proteins associated with photosynthetic pigments were clearly not upregulated for several folds in abundance (Table 2). Therefore, we concluded that the light-harvesting complex might not be the main regulatory site for leaf photosynthesis under mutual shading in the field. We know that oxygen-evolving enhancer protein 1 is an important component of the oxygen-evolving complex in PSII [26,27]. In this study, we observed that the abundance of oxygen-evolving enhancer protein was significantly downregulated because of mutual shading in the field (Table 2). It is probably disadvantageous to the stability of PSII and activity of the oxygen-evolving complex. At the same time, abundances of Fd, FNR, and putative NADH-plastoquinone oxidoreductase subunit K isoform 1 were all downregulated in plants grown under close planting conditions (Table 2), which may result in a decrease in the electron transport rate. Additionally, mutual shading also caused the downregulation in the expressions of ATP synthase and FNR (Table 2), which may limit the production of NADPH and ATP to a certain extent. Therefore, the low-light environment caused by mutual shading at high planting density caused a decline in the electron transport rate

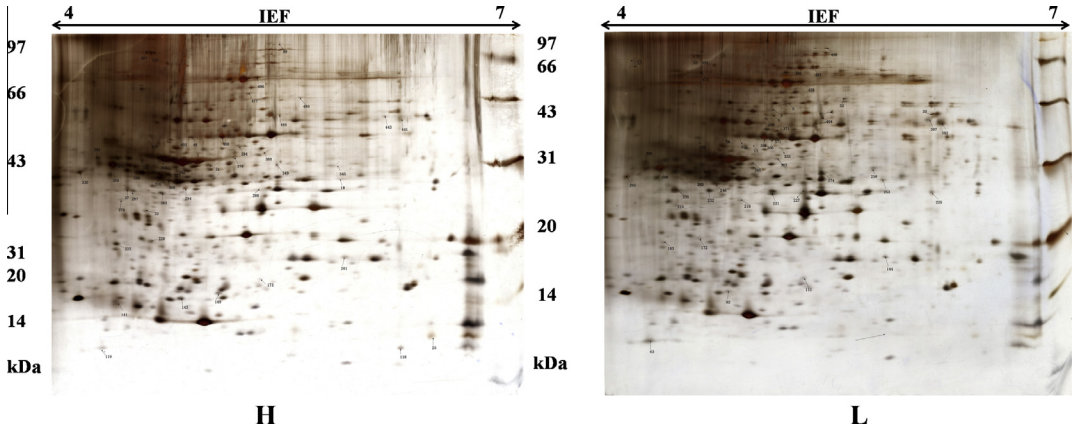

Fig. 6. Representative 2-D gels of proteins extracted from sorghum grew at the low (*L*) and high (*H*) planting densities. An equal amount of total proteins was loaded on each gel strip of 24 cm (pH 4–7). SDS–PAGE gels were used for second dimension separation after isoelectric focusing. Protein spots were visualized using coomasie brilliant blue staining. There was significant difference ($p < 0.05$) in the intensity of protein spots which were identified by MALDI Tof/Tof and the results were shown in Table 2. (For interpretation of the references to colour in this figure legend, the reader is referred to the web version of this article.)

Table 2
Changes in the expression level of proteins classified into the functional categories as light reaction, carbon metabolism, photoreceptor and photoprotection.

Spot no.	Accession no.	Protein name	Plant species	Theoretical Mw/*pI*	Experimental Mw/*pI*	Cellular location	Fold change
Light reaction							
5	gi|414870040	TPA: putative NADH-plastoquinone oxidoreductase subunit K isoform 1	Zea mays	43/5.27	48.4/4.79	Chloroplast	2.4375↑
118	gi|342316341	Photosystem I subunit VII (PSI iron-sulfur center)	Wolffiella lingulata	10/4.67	9.3/5.65	Chloroplast	↓
366	gi|225431122	PREDICTED: ferredoxin-NADP reductase, leaf isozyme, chloroplastic isoform 1	Vitis vinifera	36/5.15	41/8.91	Chloroplast	↑
368	gi|162458489	ferredoxin	Zea mays	35/5.1	41/7.5	Chloroplast	2.7084↑
392	gi|397702103	ferredoxin-NADP reductase	Saccharum hybrid cultivar GT28	38/6.32	40.5/7.53	Chloroplast	2.56617↑
11	gi|321373501	ATP synthase beta subunit	Pleurozia purpurea	34/5.04	45.1/4.84	Chloroplast	↑
232	gi|17224753	ATP synthase beta subunit	Tacca palmata	26/4.72	52.8/5.08	Chloroplast	2.01646↑
246	gi|357133129	PREDICTED: ATP synthase subunit beta, chloroplastic-like	Brachypodium distachyon	27/4.76	50.6/5.2	Chloroplast	3.69059↑
320	gi|57868948	ATP synthase beta subunit	Empetrum Hermaphroditum	31/5.73	53/5.76	Chloroplast	2.12516↑
473	gi|150035723	ATP synthase beta subunit	Phragmites australis	59/4.66	51.1/5.20	Chloroplast	↑
Carbon metabolism							
376	gi|40068128	Ribulose-1,5-bisphosphate carboxylase/oxygenase large subunit	Valeriana dioica	32/5.28	51/6.04	Chloroplast	2.19223↓
274	gi|195605636	Triosephosphate isomerase	Zea mays	29/5.49	27.3/5.53	Cytosolic	3.76662↑
398	gi|195645472	Phosphoribulokinase	Zea mays	39/5.11	46.1/5.75	Chloroplast	↑
492	gi|226506366	Sedoheptulose bisphosphatase1	Zea mays	72/4.63	42.3/6.08	Chloroplast	2.30201↑
480	gi|237652074	Sucrose synthase	Vigna luteola	61/5.27	21/5.82	Chloroplast	↑
371	gi|361738615	Granule-bound starch synthase I, partial	Solanum loxophyllum	36/5.18	37/6.33	Chloroplast	↑
397	gi|320449084	Malate dehydrogenase	Zea mays	39/6.23	36/5.76	Cytoplasmic	3.90755↑
Photoreceptor proteins							
349	gi|78217443	Cryptochrome 2	Nicotiana sylvestris	35/4.64	73.0/5.72	Nucleus	3.03321↑
372	gi|377823248	Phytochrome C, partial	Pereskiopsis gatesii	32/4.43	42/6.45	Cytosol	↓
Photoprotection							
55	gi|226499860	Stromal 70 kDa heat shock-related protein	Glycine max	73/4.6	74/5.2	Chloroplast	2.80742↑
483	gi|145388994	Chloroplast heat shock protein 70	Cenchrus americanus	62/5.4	73/5.23	Chloroplast	↑
263	gi|195619530	Oxygen-evolving enhancer protein 1	Zea mays	28/4.7	34/5.59	Chloroplast	6.69626↑

Changes in the protein expression levels are shown as fold change (↑ and ↓) of the low planting density relative to the high planting density. The large changes of protein expression are indicated in ↑ (elevated) and ↓ (decreased). The number and the names of the proteins which were identified successfully are listed and classified by the function of proteins.

and formation of assimilatory power, indicating that these two factors may be important regulatory sites for photosynthesis under mutual shading conditions in the field.

The Calvin cycle is a chain reaction, constituted of numerous enzymes. In this study, many enzymes associated with the Calvin cycle, such as triose phosphate isomerase, SBPase, and phosphoribulokinase were all downregulated in plants grown under close planting conditions (Table 2). It is well known that RuBP reacts with CO_2 to produce PGA catalyzed by Rubisco. Later, PGAld is formed in the presence of ATP and NADPH, and PGAld is then transformed into RuBP in the Calvin cycle. Our data indicated that the reproductive phases of RuBP may slow down in leaves grown under close planting conditions. The decline in the photosynthetic rate could therefore be partially attributed to depression of RuBP

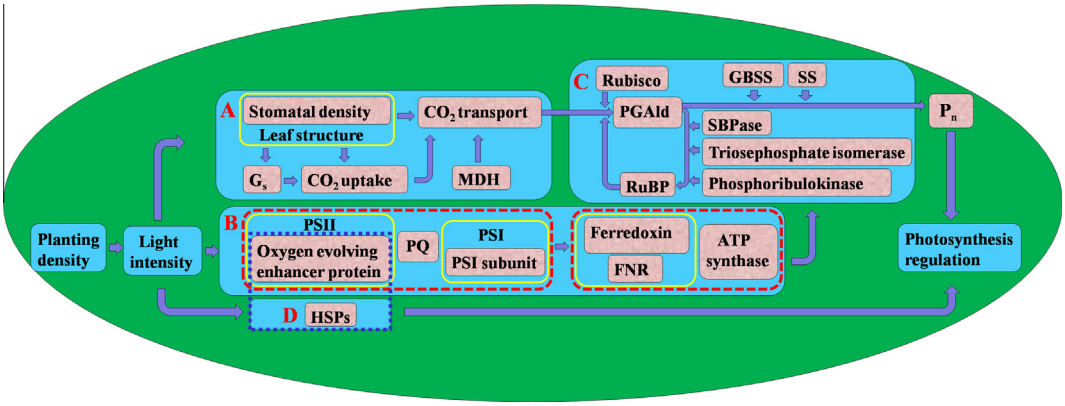

Fig. 7. Network model for photosynthesis regulation in field-grown sorghum. A: absorption and transportation of CO_2; B: electron transport and production of assimilatory power; C: enzymes related to carbon assimilation; D: photoprotective mechanisms. Abbreviations (Gs: stomatal conductance. MDH: malate dehydrogenase. PQ: plastoquinone. FNR: ferredoxin-NADP reductase. RuBP: ribulose-1, 5-bisphosphate. PGAld: 3-phosphoglyceraldehyde. SBPase: sedoheptulose-1, 7-bisphosphate phosphatase. Rubisco: RuBP carboxylase/oxygenase. GBSS: granule-bound starch synthase. SS: sucrose synthase. Hsp: heat shock protein. Pn: photosynthetic rate).

regeneration under mutual shading conditions. In addition, SS and GBSS may also be important regulatory sites for photosynthesis, reflected in the clear downregulation of their abundance under close planting conditions (Table 2). In contrast, Rubisco is commonly regarded as a key enzyme in photosynthesis [28,29]. However, the changes in Rubisco content have been controversial in previous studies. On one hand, there is a positive correlation between the Rubisco content and photosynthetic rate [29,30]. On the other hand, Ray et al. found rice to have high P_n with a low Rubisco content [31]. Recently, Li et al. report that *Suaeda salsa* seedlings maintained a high photosynthetic rate under salt stress, while Rubisco abundance was significantly downregulated [22]. Rubisco, in fact, also serves as an important storage protein [32]. In the present study, a decline in the photosynthetic rate with upregulation of Rubisco was observed under close planting conditions (Table 2). Accordingly, we concluded that Rubisco, which serves as an important functional and storage protein, may not be the rate-limiting photosynthetic step under mutual shading conditions.

Though the process of photosynthesis has been extensively studied, most previous studies have mainly focused on a few regulatory steps of light acclimation and did not reveal the potential regulatory network. In this study, under mutual shading conditions, the reduction of photosynthesis in sorghum was found to involve the regulation of leaf structure, absorption and transportation of CO_2, electron transport, assimilatory power formation, and enzymes associated with the Calvin cycle. On the basis of our results, a possible regulatory network for photosynthesis under mutual shading conditions is proposed in Fig. 7.

4.2. Effects of mutual shading on photoprotective mechanisms

Although the maximum light intensity was approximately 1343 μmol m^{-2} s^{-1} at low planting density (Fig. 2A), the expression of proteins associated with the xanthophyll cycle and antioxidant enzyme defense system was not upregulated. Therefore, regulation of protein abundance may not be the main light acclimation mechanisms in the field for the xanthophyll cycle and antioxidant enzyme defense system. Probably, the regulation of enzyme activities might be more important. Additionally, our data proved that the abundance of heat shock protein (Hsp) and oxygen-evolving enhancer protein were both downregulated at high planting density (Table 2). Moreover, accumulating evidence indicates that chloroplast Hsp is important in PSII thermotolerance, which could protect PSII and oxygen-evolving complex proteins from being damaged under heat stress [7]. At the same time, oxygen-evolving enhancer proteins are favorable to maintaining the stability of the oxygen-evolving complex [26], and its stability also plays a crucial role in protecting PSII against high temperature [27]. In our study, not only light intensity, but also air temperature, were markedly enhanced at low planting density (Fig. 2). The upregulation of Hsp and oxygen-evolving enhancer protein were clearly observed (Table 2), thus alleviating photoinhibition and photodamage. Generally, in order to improve the acclimation of crops to strong light and high temperature in the field, greater attention than previously has been paid to strengthening the xanthophyll cycle and antioxidant enzymic defense system. However, our results indicate that Hsp and oxygen-evolving enhancer protein may both play very important roles in improving strong light and high temperature tolerance in the field.

5. Conclusions

Taken together, the depression of photosynthesis in sorghum under mutual shading involves the regulation of leaf structure, absorption and transportation of CO_2, photosynthetic electron transport, production of assimilatory power, and levels of enzymes related to carbon assimilation. Additionally, heat shock protein and oxygen-evolving enhancer protein may play important roles in photoprotection in field-grown sorghum.

Acknowledgements

This study was funded by Projects of National Natural Science Foundation of China (30871455), the Knowledge Innovation Engineering of Chiese Academy of Sciences (KSCX2-EW-B-9) and Natural Science Foundation of Beijing (6122025). We also thank Ms Feng-Qin Dong for her great help in the analyzing leaf structure.

References

[1] G. Estrada-Campuzano, D.J. Miralles, G.A. Slafer, Yield determination in triticale as affected by radiation in different development phases, Eur. J. Agron. 28 (2008) 597–605.
[2] H.W. Li, D. Jiang, B. Wollenweber, T.B. Dai, W.X. Cao, Effects of shading on morphology, physiology and grain yield of winter wheat, Eur. J. Agron. 33 (2010) 267–275.
[3] P. Baldi, K. Muthuchelian, N.L. Porta, Leaf plasticity to light intensity in Italian cypress (*Cupressus sempervirens L.*): adaptability of a mediterranean conifer cultivated in the Alps, J. Photochem. Photobiol. B 117 (2012) 61–69.
[4] C.D. Jiang, X. Wang, H.Y. Gao, L. Shi, W.S. Chow, Systemic regulation of leaf anatomical structure, photosynthetic performance, and high-light tolerance in sorghum, Plant Physiol. 155 (2011) 1416–1424.

[5] J.M. Anderson, Photoregulation of the composition, function, and structure of thylakoid membranes, Ann. Rev. Plant Physiol. 37 (1986) 93–136.
[6] P.E.R. Marchiori, E.C. Machado, R.V. Ribeiro, Photosynthetic limitations imposed by self-shading in field-grown sugarcane varieties, Field Crop. Res. 155 (2014) 30–37.
[7] S.A. Heckathorn, C.A. Downs, T.D. Sharkey, J.S. Coleman, The small, methioine-rich chloroplast heat-shock protein protects photosystem II electron transport during heat stress, Plant Physiol. 116 (1998) 439–444.
[8] E. Janik, W. Maksymiec, W.I. Gruszecki, The photoprotective mechanisms in *Secale cereale* leaves under Cu and high light stress condition, J. Photochem. Photobiol. B 101 (2010) 47–52.
[9] M. Naramoto, S.I. Katahata, Y. Mukai, Y. Kakubari, Photosynthetic acclimation and photoinhibition on exposure to high light in shade-developed leaves of *Fagus crenata* seedlings, Flora 201 (2006) 120–126.
[10] J.Y. Yamazaki, K. Kamata, E. Maruta, Seasonal changes in the excess energy dissipation from photosystem II antennae in overwintering evergreen broad-leaved tress *Quercus myrsinaefolia* and *machilus thunbergii*, J. Photochem. Photobiol. B 104 (2011) 348–356.
[11] Y.M. Deng, Q.S. Shao, C.C. Li, X.Q. Ye, R.S. Tang, Differential responses of double petal and multi petal jasmine to shading: II. Morphology, anatomy and physiology, Sci. Hortic. 144 (2012) 19–28.
[12] M.J. Berenguer, J.M. Faci, Sorghum (*Sorghum Bicolor L. Moench*) yield compensation processes under different plant densities and variable water supply, Eur. J. Agron. 15 (2001) 43–55.
[13] S.J. Zhang, X. Liao, C.L. Zhang, H.J. Xu, Influences of plant density on the seed yield and oil content of winter oilseed rape (*Brassica napus* L.), Ind. Crop. Prod. 40 (2012) 27–32.
[14] B.G. Wherley, D.S. Gardner, J.D. Metzger, Tall fescue photomorphogenesis as influenced by changes in the spectral composition and light intensity, Crop. Sci. 45 (2005) 562–568.
[15] H. Smith, G.C. Whitelam, The shade avoidance syndrome: multiple responses mediated by multiple phytochromes, Plant Cell Environ. 20 (1997) 840–844.
[16] B. Genty, J.M. Briantais, N.R. Baker, The relationship between the quantum yield of photosynthetic electron transport and quenching of chlorophyll fluorescence, Biochim. Biophys. Acta 990 (1989) 87–92.
[17] R.J. Porra, W.A. Thompson, P.E. Kriedemann, Determination of accurate extinction coefficients and simultaneous equations for assaying chlorophylls *a* and *b* extracted with four different solvents: verification of the concentration of chlorophyll standards by atomic absorption spectroscopy, Biochim. Biophys. Acta 975 (1989) 384–394.
[18] S.A. Coupe, B.G. Palmer, J.A. Lake, S.A. Overy, K. Oxborough, F.I. Woodward, J.E. Gray, W.P. Quick, Systemic signalling of environmental cues in *Arabidopsis* leaves, J. Exp. Bot. 57 (2006) 329–341.
[19] J.F. Thain, Curvature correction factors in the measurement of cell surface areas in plant tissues, J. Exp. Bot. 34 (1983) 87–94.
[20] C. Damerval, D.D. Vienne, M. Zivy, H. Thiellement, Technical improvements in two-dimensional electrophoresis increase the level of genetic variation detected in wheat-seedling proteins, Electrophoresis 7 (1986) 52–54.
[21] L.S. Ramagli, Quantifying protein in 2-D PAGE solubilization buffers, Methods Mol. Biol. 112 (1999) 99–103.
[22] W. Li, C.Y. Zhang, Q.T. Lu, X.G. Wen, C.M. Lu, The combined effect of salt stress and heat shock on proteome profiling in *Suaeda salsa*, J. Plant Physiol. 168 (2011) 1743–1752.
[23] P.X. Fan, J.J. Feng, P. Jiang, X.Y. Chen, H.X.G.D.L. Bao, L.L. Nie, D. Jiang, S.L. Lv, T.Y. Kuang, Y.X. Li, Coordination of carbon fixation and nitrogen metabolism in Salicornia europaea under salinity: comparative proteomic analysis on chloroplast proteins, Proteomics 11 (2011) 4346–4367.
[24] I. Terashima, Y. Inoue, Palisade tissue chloroplasts and spongy tissue chloroplasts in spinach: biochemical and ultrastructural differences, Plant Cell Physiol. 26 (1985) 63–75.
[25] P. Sowiński, J. Szczepanik, P.E.H. Minchin, On the mechanism of C_4 photosynthesis intermediate exchange between Kranz mesophyll and bundle sheath cells in grasses, J. Exp. Bot. 59 (2008) 1137–1147.
[26] M. Suorsa, E.M. Aro, Expression, assembly and auxiliary functions of photosystem II oxygen-evolving proteins in higher plants, Photosynth. Res. 93 (2007) 89–100.
[27] M. Busheva, I. Tzonova, K. Stoitchkova, A. Andreeva, Heat-induced reorganization of the structure of photosystem II membranes: role of oxygen evolving complex, J. Photochem. Photobiol. B 117 (2012) 214–221.
[28] A.E. Carmo-Silva, M.A. Gore, P. Andrade-Sanchez, A.N. French, D.J. Hunsaker, M.E. Salvucci, Decreased CO_2 availability and inactivation of Rubisco limit photosynthesis in cotton plants under heat and drought stress in the field, Environ. Exp. Bot. 83 (2012) 1–11.
[29] Y. He, C.L. Yu, L. Zhou, Y. Chen, A. Liu, J.H. Jin, J. Hong, Y.H. Qi, E.A. Jiang, Rubisco decrease is involved in chloroplast protrusion and Rubisco-containing body formation in soybean (*Glycine max*.) under salt stress, Plant Physiol. Bioch. 74 (2014) 118–124.
[30] L.D. Zhang, L.X. Zhang, J.L. Sun, Z.X. Zhang, H.Z. Ren, X.L. Sui, Rubisco gene expression and photosynthetic characteristics of cucumber seedlings in response to water deficit, Sci. Horti. 161 (2013) 81–87.
[31] D. Ray, M.S. Sheshshayee, K. Mukhopadhyay, H. Bindumadhava, T.G. Prasad, M.U. Kumar, High nitrogen use efficiency in rice genotypes is associated with higher net photosynthetic rate at lower Rubisco content, Biol. Plant. 46 (2003) 251–256.
[32] C.R. Warren, E. Dreyer, M.A. Adams, Photosynthesis-Rubisco relationships in foliage of *Pinus sylvestris* in response to nitrogen supply and the proposed role of Rubisco and amino acids as nitrogen stores, Trees 17 (2003) 359–366.